Journal of Catalysis 286 (2012) 95–102

Contents lists available at SciVerse ScienceDirect

Journal of Catalysis

journal homepage: www.elsevier.com/locate/jcat

DFT investigation of hydroperoxide decomposition over copper and cobalt sites within metal-organic frameworks

Patrick Ryan, Ivan Konstantinov, Randall Q. Snurr *, Linda J. Broadbelt *

Department of Chemical and Biological Engineering, Northwestern University, 2145 Sheridan Road, Evanston, IL 60208, United States

ARTICLE INFO

Article history:
Received 28 June 2011
Revised 19 September 2011
Accepted 21 October 2011
Available online 21 November 2011

Keywords:
Metal-organic framework
Catalysis
Peroxide decomposition
DFT
Haber–Weiss cycle

ABSTRACT

Experimental results in the literature show that two metal-organic frameworks (MOFs) containing copper and cobalt nodes are active for hydroperoxide decomposition, which is an important reaction in autoxidation processes. Density functional theory (DFT) calculations reported here for these systems suggest that the metal sites in the interior of these MOFs are not the active sites for this type of reaction due to the steric effects of the adjacent linkers. This implies that the experimental catalysis observed may occur on the exterior surface of the MOF crystals. Additional calculations with a copper paddlewheel node show that, despite being able to form complexes with hydroperoxides, the metal sites in copper paddlewheels do not catalyze hydroperoxide decomposition. Preliminary calculations involving undercoordinated metal atoms as a model for metal sites on the MOF exterior crystal surface suggest that these sites could be catalytically active.

1. Introduction

Metal-organic frameworks [1–5], or MOFs, are a new class of nanoporous materials composed of metal cations connected by organic linkers. These materials are synthesized in a self-assembly process yielding stable, porous, and crystalline frameworks. Large surface areas, open pores, low densities, and high thermal stabilities are a few of their attractive properties. The ability to tailor the pore environment with different linkers and maintain ordered, periodic pores has attracted much interest in MOFs for hydrogen storage [6–8], gas separation [9,10], and more recently catalysis [11–15].

There are four distinct ways in which MOFs can be used for catalysis [16], as shown in Fig. 1. The first is to use unsaturated metal sites that are sometimes present at the nodes or corners of these materials; for example, Schlichte et al. [17] showed that unsaturated square planar copper sites in HKUST-1 could catalyze a cyanosilylation reaction with coordinated benzaldehyde. Choomwattana et al. [18] used hybrid quantum/classical computational methods to predict that a concerted, single-step reaction between formaldehyde and propylene could be catalyzed over copper node sites in MOF-11. Another strategy is to incorporate active sites within the organic linkers. Cho et al. [13] immobilized an active Mn-salen catalyst as an organic linker within a mixed-ligand MOF and found that it catalyzes enantioselective epoxidation of an olefin substrate. Whereas homogeneous salen catalysts are prone to deactivation due to formation of μ-oxo dimers, the salen MOF catalyst exhibited close to constant reactivity over the course of the experiment and could be reused for subsequent reactions. Gascon et al. [19] recently used amine-functionalized MOFs, namely IRMOF-3 and amino-functionalized MIL-53, to catalyze Knoevenagel condensation reactions. The third strategy is to use linkers or metal sites within MOFs as attachment points for catalysts. Banerjee et al. [20] post-synthetically modified the MIL-101 MOF [21] by coordinating chiral organic catalysts to unsaturated metal nodes and noticed these heterogenized catalysts resulted in much higher enantiomeric excess of aldol reaction products relative to the homogeneous chiral catalyst in solution. Finally, MOFs can be used for the encapsulation of other active catalysts; for example, Sun et al. [22] recently incorporated polyoxometalate species within HKUST-1 and found that these species selectively occupied one of the larger type pores within the structure. They discovered that the hybrid catalyst was active for ethyl acetate hydrolysis and that its activity compared well with other common catalysts for this reaction. Alkordi et al. [23] incorporated porphyrins within the pores of a zeolite-like MOF and demonstrated the catalytic activity of the encapsulated porphyrins for cyclohexane oxidation.

Capitalizing on the idea of using open metal sites in MOFs for catalysis, Llabrés i Xamena et al. [24] demonstrated that two copper- or cobalt-containing MOFs were active for tetralin oxidation to ketone and alcohol derivatives, as shown in Fig. 2. The basic free radical mechanism underlying this chemistry is well understood, where hydrocarbons are initially oxidized to hydroperoxides. It was proposed that the MOFs catalyze the hydroperoxide decomposition reactions, following the Haber–Weiss cycle. In this cycle, metal

* Corresponding authors. Fax: +1 847 491 3728.
E-mail addresses: snurr@northwestern.edu (R.Q. Snurr), broadbelt@northwestern.edu (L.J. Broadbelt).

0021-9517/$ - see front matter © 2011 Elsevier Inc. All rights reserved.
doi:10.1016/j.jcat.2011.10.019

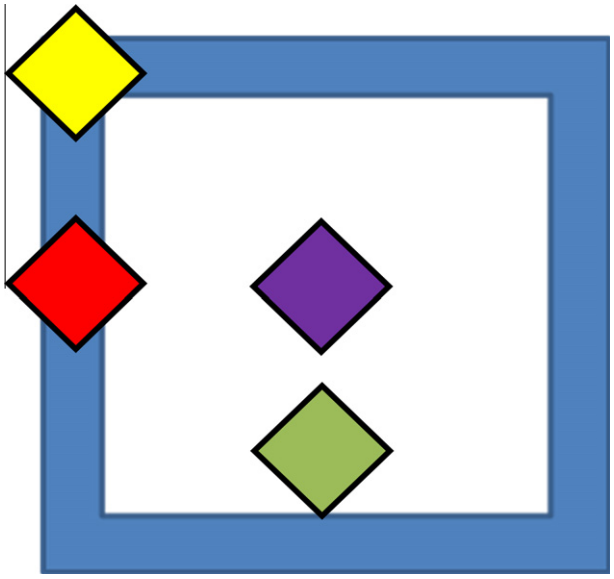

Fig. 1. Catalytic sites can be introduced into MOFs in four distinct ways: unsaturated metal sites at the nodes (yellow), homogeneous catalysts incorporated as part of the framework (red), catalysts attached to either nodes or linkers (green), and supported or encapsulated catalysts (purple). (For interpretation of the references to color in this figure legend, the reader is referred to the web version of this article.)

cations undergo oxidation and reduction to decompose hydroperoxides into alkoxy and peroxy radical species, respectively:

$$ROOH + M^{n+} \rightarrow RO^{\cdot} + OH^{-} + M^{(n+1)+}$$
$$ROOH + M^{(n+1)+} \rightarrow ROO^{\cdot} + H^{+} + M^{n+}$$

The presence of the MOF prevented buildup of the intermediate hydroperoxide, in contrast to the reaction in the absence of the MOF [24]. However, the exact role of the MOF and its interaction with reactive intermediates are yet to be fully understood.

In related chemistry, Moden et al. [25] suggested that radical species during cyclohexane auto-oxidation over a MnAlPO-5 catalyst remained bound as adsorbed intermediates and that ROOH decomposition over Mn^{2+} sites was a kinetically-relevant step. Gomez-Hortiguela et al. [26] noted the importance of redox activity and coordinative unsaturation of MnAlPO-5 sites for oxidation of both hydrocarbons and hydroperoxide species. For homogeneous systems, Zabarnick and Phelps [27] also proposed that ·OH radicals could remain bound to metal cations after oxygen–oxygen bond cleavage during hydroperoxide decomposition. Turra et al. [28] used quantum mechanics to map a Haber–Weiss reaction cycle over the homogeneous catalyst cobalt(II) acetylacetonate. By analogy, the open metal sites in the MOFs could play similar roles. While commercial processes for auto-oxidation have used copper and cobalt salts for some time, only a few examples exist in which researchers used computational methods to investigate oxidation reactions over these metal salts [27–29].

In this article, we investigate the decomposition of hydroperoxides over the two MOFs studied by Llabrés i Xamena et al. using quantum chemical calculations. The cobalt-containing MOF (denoted here simply as Co-MOF), composed of Co^{2+} cations and anionic phenylimidazolate linkers, has a sodalite-type structure and is also known as zeolitic imidazolate framework 9 (ZIF-9) developed by the Yaghi group [30]. The cobalt atoms in this MOF are coordinated in a tetrahedral geometry with the adjacent linkers. The copper-containing MOF (Cu-MOF) [31] is composed of Cu^{2+} cations and 2-hydroxypyrimidinolate linkers in a 1:2 molar ratio. Copper sites are in a near-square planar configuration, which leaves them coordinatively unsaturated and able to interact with guest molecules. Additionally, we investigate the copper paddlewheel structure, which is a common structural motif in several MOFs, including HKUST-1 [32] and the NOTT series [33].

2. Computational methods

In this study, representative clusters were extracted from the MOF crystal structures around the active sites. For Co-MOF, one cobalt atom with four surrounding linkers was chosen as the model, but to reduce the computational cost, smaller imidazolate linkers were used instead of the phenylimidazolate linkers, as shown in Fig. 3a. For Cu-MOF, one copper atom and four 2-hydroxypyrimidinolate linkers were modeled (Fig. 3b). In the periodic MOF, the linkers of both MOFs are anionic and bound at both ends by metal cations. In our cluster models, the four boundary atoms of the cluster (where the next metal atom would occur in the periodic structure) were saturated with protons. This choice renders the metal–nitrogen bonds between all four linkers and the central metal atom equivalent and gives each cluster a charge of 2+. The copper paddlewheel model was composed of two copper atoms coordinated to four acetate groups, yielding a charge neutral cluster. See Fig. 3. 1-Phenylethylhydroperoxide, the hydroperoxide of ethylbenzene, was studied as the reactant. Given the presence of a benzylic carbon, it is a suitable model of tetralin, which should undergo similar auto-oxidation and decomposition reactions.

Density functional theory (DFT) calculations with Becke's three-parameter hybrid exchange functional (B3) [34] and the correlation functional of Lee, Yang, and Parr (LYP) [35] were performed. To select a basis set, calculated bond energies using several methods for

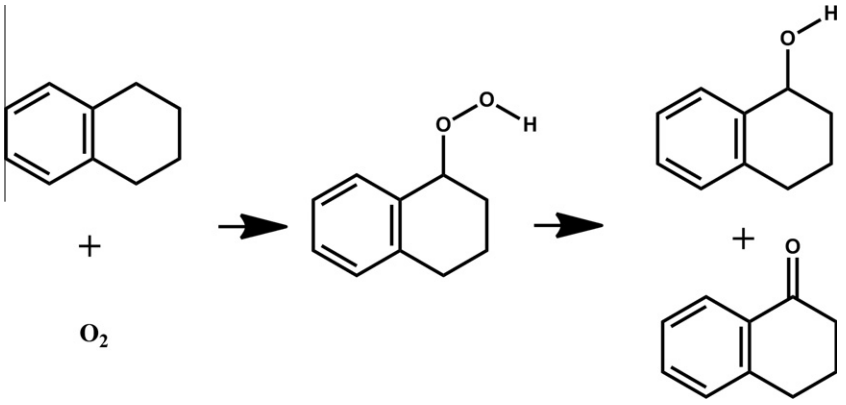

Fig. 2. Auto-oxidation reaction scheme of tetralin in the presence of dioxygen to alcohol and ketone derivatives.

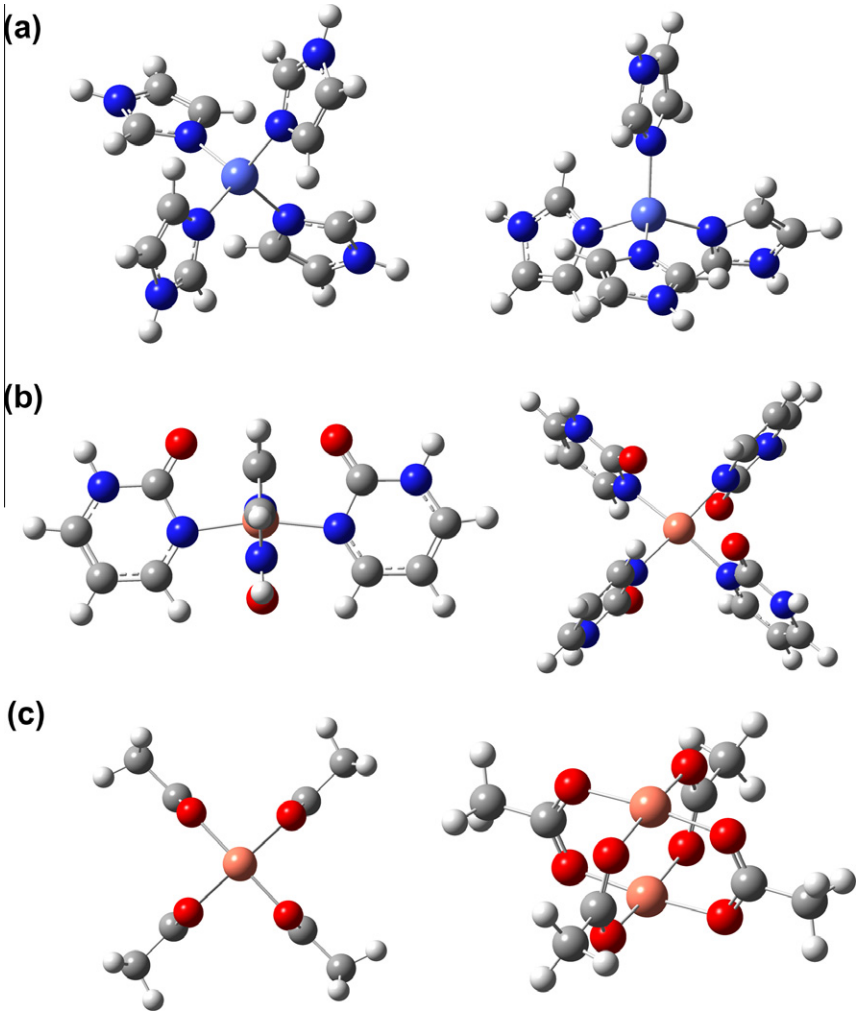

Fig. 3. Representative metal clusters taken from (a) Co-MOF, (b) Cu-MOF, and (c) copper paddlewheel. Two views of each cluster are shown. Carbon, nitrogen, oxygen, hydrogen, cobalt, and copper atoms are gray, dark blue, red, white, light blue, and peach, respectively. (For interpretation of the references to color in this figure legend, the reader is referred to the web version of this article.)

O–O and O–H bonds in ethylhydroperoxide were compared to experimental values [36,37] of saturated alkyl hydroperoxides (see Supplementary material). Based on a compromise of speed and accuracy, we adopted the following procedure: First, geometry optimizations were performed with the TZVP [38] basis set for metal atoms and the 6-31G(d,p) [39] basis set for all other atoms (hereafter referred to as TZVP/6-31G(d,p)). These were followed by single-point energy calculations with a TZVP basis set for metal atoms and the 6-311G(d,p) [40] basis set for all other atoms (TZVP/6-311G(d,p)). This choice was also motivated by previous research, which found that using triple-ζ basis sets for copper and at least double-ζ basis sets with polarization for the ligands bound to copper along with the B3LYP functional is a reasonable choice to describe the electronic structure of a square planar copper complex [41]. Additional work has also used the B3LYP functional to investigate the coordination environments surrounding Cu(II) complexes [42,43]. Free energy corrections were calculated at 298 K using the rigid rotor, harmonic oscillator approximation for vibrational frequencies at the TZVP/6-31G(d,p) level of theory, which were then added to the electronic energies of each intermediate at the TZVP/6-311G(d,p) level of theory to give the corresponding Gibbs free energy values.

All calculations were done with Gaussian 09 [44]. The MOF clusters were initially taken from the crystal structures. Boundary protons were added as described above, and the clusters were fully optimized. Stable intermediates for the proposed catalytic cycle were then sought as minima on the electronic energy surface, and searches for the transition states (TS) connecting the minima were conducted. All TSs were identified as having one negative frequency, and internal reaction coordinate (IRC) calculations were performed to verify that the TSs connect the reactants and products of interest. Dihedral scans were performed to ensure that the lowest energy conformers were determined for all intermediates. Basis set superposition error (BSSE) was calculated using the counterpoise method [45] and incorporated into the energies of all minima and transition states along the reaction coordinate.

The copper paddlewheel is an example of a metal–ligand complex that displays antiferromagnetic character. In these systems, the ground electronic state is an open-shell singlet, where the unpaired electrons on the two copper atoms have opposite spin. Tafipolsky et al. [46] have calculated the difference in energy between the antiferromagnetic singlet and the triplet state of a copper acetate monohydrate to be 1.06 kcal/mol. This value was estimated using a broken-spatial-symmetry (BS) approach with DFT methods [47], which resulted in a highly spin-contaminated BS solution [48]. Since the BS approach with DFT can only estimate the energy of the antiferromagnetic singlet and the energy difference between the antiferromagnetic singlet and triplet state is

sufficiently small, all calculations here involving the paddlewheel assumed the triplet state as the ground state. This approximation is computationally more straightforward and should not significantly affect the reaction coordinate. Further justification is provided in the Supplementary material.

The reaction coordinate involves breaking the oxygen–oxygen bond of ethylbenzene hydroperoxide. During bond cleavage, the multiplicity of the system changes. The point of spin crossing was estimated using a code developed by Harvey et al. [49], which iteratively solves for a geometry that has an identical electronic energy for both spin states. Single-point calculations were then performed at the TZVP/6-311G(d,p) level of theory for the geometry determined at the lower level of theory using the code. Since the single-point energies, free energy corrections, and BSSE corrections for each spin state are different, the point of spin crossing in the reaction coordinate is reported as a range of energies. Although this bond breaking results in a spin-contaminated solution for the low-spin state, it allows an estimation of the point of spin crossing without resorting to more computationally expensive methods, such as multi-configuration self-consistent field (MCSCF) calculations.

3. Results and discussion

Based on the Haber–Weiss cycle and evidence in the literature that intermediates may remain bound to the catalyst metal atoms during similar reactions [25], the following reaction mechanism for hydroperoxide decomposition over metal sites in MOFs was proposed:

$$M^{2+} + ROOH \rightarrow [M^{2+} - ROOH] \quad (1)$$

$$[M^{2+} - ROOH] \rightarrow [M(OH)]^{2+} + RO^{\cdot} \quad (2)$$

$$[M(OH)]^{2+} + ROOH \rightarrow M^{2+}(H_2O) + ROO^{\cdot} \quad (3)$$

$$M^{2+}(H_2O) \rightarrow M^{2+} + H_2O \quad (4)$$

$$\text{Net reaction: } 2ROOH \rightarrow RO^{\cdot} + ROO^{\cdot} + H_2O \quad (5)$$

The proposed catalytic cycle begins with forming a bound complex involving the metal center and the hydroperoxide species, which is followed by oxygen–oxygen bond cleavage. After RO· leaves, another hydroperoxide species can enter and react to form a bound water molecule and ROO·. The catalytic cycle is complete when water desorbs. Similar to the Haber–Weiss cycle, both alkoxy and peroxy radical species are formed. Water is formed instead of H^+ and OH^-, since the hydrocarbon substrate, which is also the solvent, would not effectively stabilize ionic species.

Initially, the cobalt cluster was held fixed and an ethylbenzene hydroperoxide molecule was placed nearby and optimized. Starting from various initial configurations, the hydroperoxide always left the metal site, suggesting that the metal was too sterically protected to interact with guest molecules of this size (Fig. 4a). The product complex of reaction (2) was also sought, but now allowing the cluster to fully relax. The ·OH species did form a strong interaction with the cobalt atom, but this involved substantial geometric rearrangement, as shown in Fig. 4b. The cobalt atom and its ligands reorganized into a trigonal bipyramidal structure, which is not compatible with the extended MOF structure. These two results suggest that decomposition of tetralin hydroperoxide by metal atoms inside the pores of Co-MOF is unlikely.

For the Cu-MOF, DFT calculations also revealed that the linkers shield the copper metal atom from interacting with ethylbenzene hydroperoxide. In Fig. 5a, when the copper atom and four adjacent linkers were fixed and the hydroperoxide molecule was initially placed in close proximity to the metal, geometry optimization resulted in the reactant moving further away from the metal site. To explore the effect of framework flexibility on this behavior, a larger cluster that included secondary copper atoms bonded to the primary linkers was created. The secondary copper atoms were terminated with ammonia molecules, and during the optimization, the secondary copper and nitrogen atoms of the ammonia molecules were fixed at their crystallographic coordinates in order for the cluster to be compatible with the extended MOF structure. The primary copper atom and its linkers were allowed to relax in the presence of the hydroperoxide reactant, while holding the secondary copper atoms and terminating ammonia molecules fixed. Despite this increased cluster flexibility, the hydroperoxide species

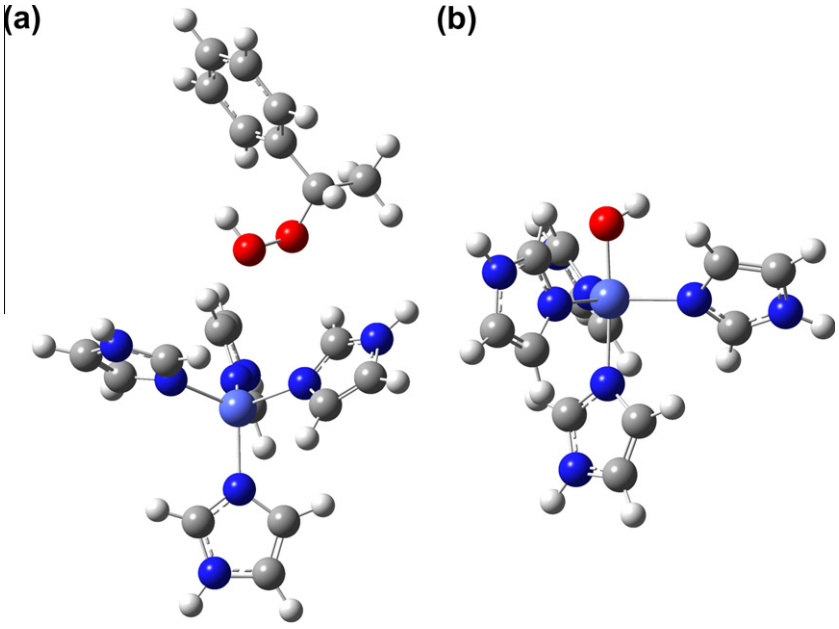

Fig. 4. (a) Optimized structure of ethylbenzene hydroperoxide (ROOH) in the presence of a fixed tetrahedral cobalt cluster. (b) Fully optimized structure of the cobalt cluster in the presence of ·OH.

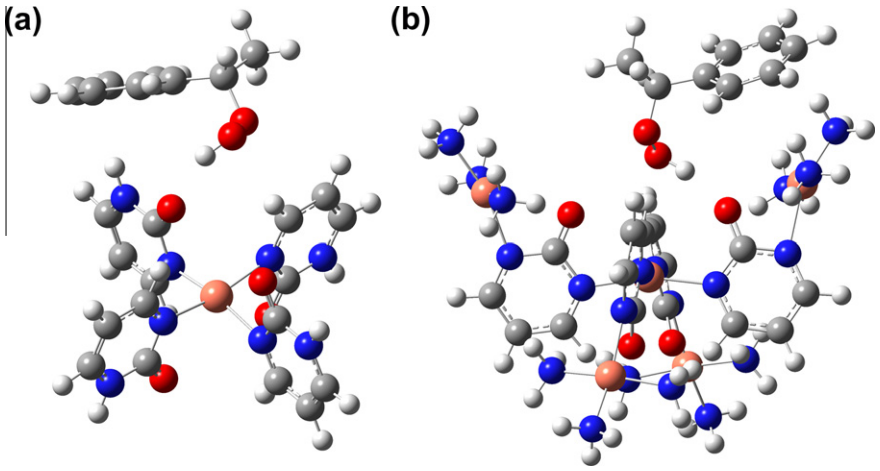

Fig. 5. (a) Optimized structure of ethylbenzene hydroperoxide (ROOH) in the presence of a fixed square planar copper cluster. (b) Optimized structure of ROOH species in the presence of an enlarged cluster with secondary copper atoms terminated with ammonia molecules.

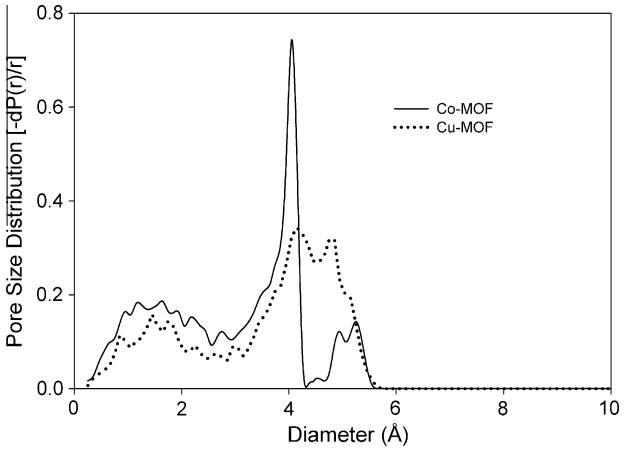

Fig. 6. Pore size distributions for Co-MOF and Cu-MOF calculated from the crystal structures.

again left the primary copper site during optimization, suggesting that complexation of the metal and ethylbenzene hydroperoxide is not energetically favorable in Cu-MOF (Fig. 5b). Although greater flexibility might be investigated with an even larger cluster, the resulting system would be too computationally expensive at this level of theory. As for the Co-MOF, our results suggest that the metal sites in Cu-MOF cannot catalyze hydroperoxide decomposition due to steric effects imposed by the linkers.

These results prompted us to examine the pore sizes of the two MOFs more carefully. The largest sphere that can fit inside Co-MOF is quoted as 4.31 Å in the literature, taking into account the sizes of the framework atoms [30]. The pore size distribution of Co-MOF based on the crystal structure was calculated using the method of Gelb and Gubbins [50] and is displayed in Fig. 6 (see Supplementary material for atomic diameter values). Similar to the literature findings, a sharp peak corresponding to a pore diameter of 4.1 Å is found. The slight difference from the literature value of 4.31 Å can be attributed to the different estimates of the van der Waals diameter of atomic hydrogen (1.2 Å versus 1.43 Å for this calculation). Additionally, according to the calculated pore size distribution, the largest sphere that can fit inside the framework is 5.6 Å, which is larger than was previously reported. Upon examination of the desolvated crystal structure [30], it is clear that there is an additional cavity not previously discussed, which is defined by six of the phenylimidazolate linkers. In order for tetralin to diffuse into the MOF crystal and access an interior cavity, it would need to pass through an opening, or pore window, that is narrower than the 5.6-Å cavity. We estimate that the pore windows connecting these cavities are only ~3 Å. Since the kinetic diameter of ethylbenzene is approximately 5.85 Å [51], the larger tetralin molecule must have a kinetic diameter equal or greater than 5.85 Å, and its hydroperoxide would be slightly larger still. The small cavity and pore window size of Co-MOF indicate that tetralin or its hydroperoxide derivative probably cannot fit inside. Our pore size distribution calculations assume that the framework atoms are fixed at their crystallographic coordinates. Previous work [52,53] finds that framework flexibility in MOFs can allow molecules to diffuse through pores that are smaller than the kinetic diameters of the molecules, although it is not clear whether this would be true for such a large difference between the molecule size (~6 Å) and the window size (~3 Å).

For Cu-MOF, the original synthesis paper quotes the pores as 8.1 Å in diameter, with connecting cavities of ~14 Å [31]. Upon examination of the desolvated crystal structure, we calculate the distance between two oxygen atoms of organic linkers that oppose one another in an interior pore window to be 8.07 Å, in agreement with the value of 8.1 Å. However, this distance does not account for the van der Waals diameter of atomic oxygen; if a diameter of 3.03 Å for atomic oxygen is assumed, then the size of this particular pore window is estimated to be only 5.04 Å. In regard to the 14-Å cavity size, it is unclear how this value was determined. Llabrés i Xamena et al. [24] mention that a Pd-containing MOF [54], which is structurally analogous to the Cu-MOF, has two distinct hexagonal windows with free openings of 4.8 and 8.8 Å, respectively. In the original synthesis paper [54], it is unclear how these values were determined. In order to clarify these different reports, the pore size distribution of Cu-MOF based on the crystal structure was also calculated and is included in Fig. 6. As the graph shows, the largest sphere that can fit inside the pores has a diameter of 5.7 Å, which is smaller than the kinetic diameter of ethylbenzene or tetralin. However, the pore windows into this cavity are only 5.04 Å, as described above. This suggests that diffusion of tetralin and its oxidation products through the pores of Cu-MOF would be severely restricted. The combination of the pore size analysis and the DFT results showing that the reactants cannot access the interior metal sites suggests that the catalysis of tetralin observed experimentally for Co-MOF and Cu-MOF may occur on the exterior crystal surface.

The interaction of ethylbenzene hydroperoxide with the copper paddlewheel structure was also examined. In contrast to Co-MOF

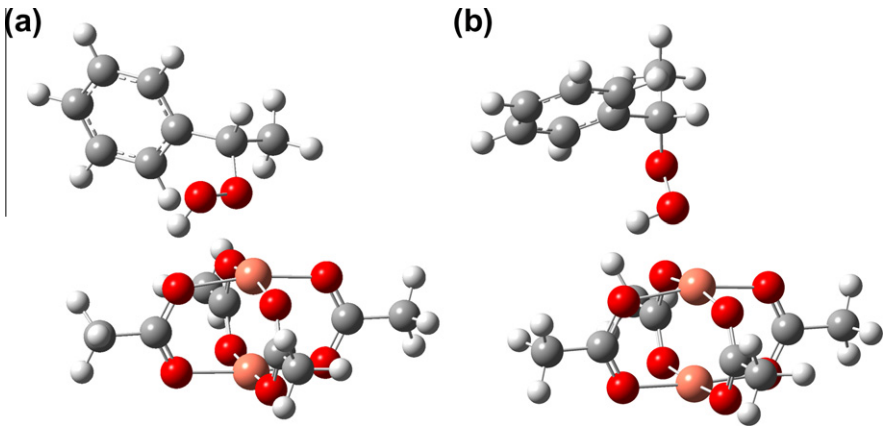

Fig. 7. Bound complexes of ethylbenzene hydroperoxide with the Cu paddlewheel structure: (left) Pad(R**O**OH) and (right) Pad(RO**O**H).

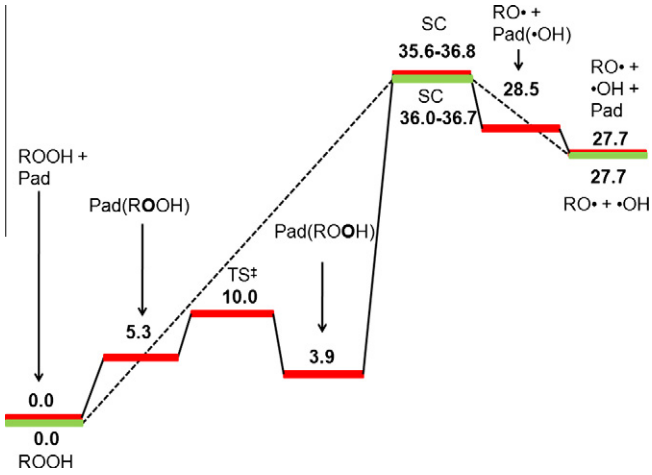

Fig. 8. Gibbs free energy along the reaction coordinate for oxygen–oxygen bond cleavage of ethylbenzene hydroperoxide (ROOH) over a copper paddlewheel (abbreviated "Pad") (red) and in the gas phase (green). TS‡ and SC denote transition state and spin crossing, respectively. All energies are in kcal/mol. (For interpretation of the references to color in this figure legend, the reader is referred to the web version of this article.)

and Cu-MOF, the hydroperoxide species is able to form complexes with the copper atoms of the paddlewheel structure, since the metal site is not sterically shielded by its surrounding linkers. In these complexes, the copper atom can be bound to either the oxygen atom adjacent to the R group (R**O**OH) or the distal oxygen atom of the hydroperoxide (RO**O**H), as shown in Fig. 7. Once the complex is formed, the hydroperoxide can undergo oxygen–oxygen bond cleavage. Fig. 8 displays the reaction coordinate for this reaction over the copper paddlewheel, as well as the reaction in the gas phase. As previously mentioned, this bond cleavage involves a point of spin crossing, where the electronic state changes from triplet to quintet (oxygen–oxygen bond distance of approximately 1.98 Å). This point on the reaction coordinate for the paddlewheel is estimated to lie 35.6–36.8 kcal/mol higher in Gibbs free energy than the infinitely separated reactants and is compared to the point of spin crossing for oxygen–oxygen bond cleavage of ethylbenzene hydroperoxide in the gas phase, which was estimated using the same technique. Since the point of spin crossing for the gas-phase reaction is estimated to be 36.0–36.7 kcal/mol higher in free energy than the stable ethylbenzene hydroperoxide, the paddlewheel does not appear to significantly catalyze the decomposition of hydroperoxides.

In the traditional Haber–Weiss cycle, a metal cation is oxidized in the first step and subsequently reduced to regenerate the catalytic species. Copper is suggested to switch between the 1+ and 2+ oxidation states during this cycle [27]. In the case of the copper paddlewheel, whose copper atoms are in a 2+ oxidation state, oxidation of the metal is unlikely due to the relative instability of Cu^{3+} species. Examination of the copper Mulliken charge over the reaction coordinate suggests that the oxidation state of the copper atom is invariant during the reaction cycle. In the bare paddlewheel, each copper atom has a charge of +0.63. In the complexes involving the hydroperoxide, the Mulliken charge of the copper atom nearest to the hydroperoxide is +0.69 and +0.65 for the two complexes shown in Fig. 7. Even after oxygen–oxygen bond cleavage, when the ·OH species is sitting atop the paddlewheel, the Mulliken charge of the copper nearest to ·OH is +0.64, suggesting that no charge transfer between the copper and oxygen atoms has occurred. Similarly, the Mulliken charges of the oxygen atoms surrounding this copper atom in the paddlewheel vary only slightly among these complexes, with values ranging from −0.414 to −0.487. Additionally, the preservation of the square planar structure of the paddlewheel is further evidence for Cu^{2+} oxidation states within the paddlewheel. For these reasons, the product of reaction 2 in our proposed cycle is written as $[M(OH)]^{2+}$ instead of $M^{3+}(OH^-)$, since copper cannot be oxidized in this system to a 3+ oxidation state.

To investigate the possibility that tetralin hydroperoxide decomposition might occur at active sites on the external surface of the MOF crystals, a model was created for a copper site at the edge of the Cu-MOF crystal. The exact geometries of these sites are not known, but there is a strong possibility that undercoordinated metal sites might be present [55,56]. By an undercoordinated metal site, we are describing a metal atom that is both part of the MOF and is missing at least one organic linker in its coordination environment. During synthesis, it is possible that these sites can become occupied with solvent molecules. In order to create a representative surface metal site of Cu-MOF, a cluster was created, in which a copper atom was coordinated to three organic linkers and a water molecule, since the synthesis conditions of Cu-MOF require an aqueous amine solution [31]. The cluster was allowed to fully relax with no geometrical constraints. As seen in Fig. 9, the water molecule coordinates to the copper atom to form a near-square planar geometry similar to that in the MOF interior. Using this cluster as a starting point (and allowing the cluster to relax), the reaction coordinate was comprehensively mapped and is plotted in Fig. 10. In the first step, the cluster exchanges the water molecule for the ROOH species. Next, the oxygen–oxygen bond of the ROOH species is lengthened and eventually broken. This point of spin crossing is estimated to lie about 18.7 kcal/mol in free energy above the initial reactants. This barrier is significantly less than that of the gas-phase reaction, which requires 36.0–36.7 kcal/mol of free energy to break the oxygen–oxygen bond of the

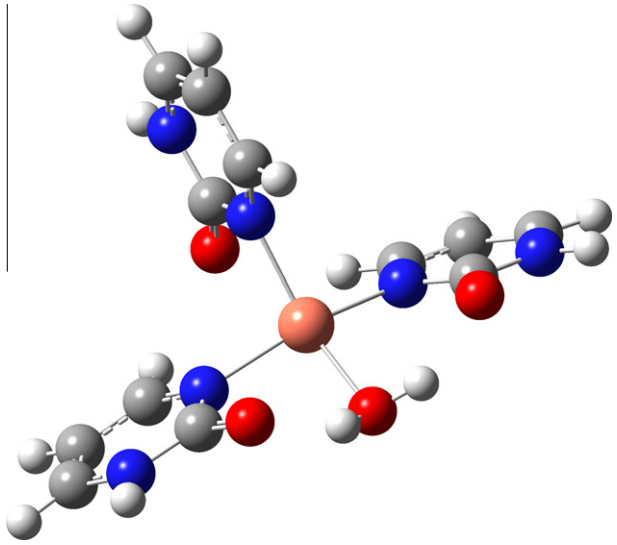

Fig. 9. Model of a possible undercoordinated metal–ligand cluster on the exterior of a Cu-MOF crystal with three organic linkers and one water molecule. Linkers on the exterior of MOF crystals will likely not be as structurally confined as those in the interior of the MOF.

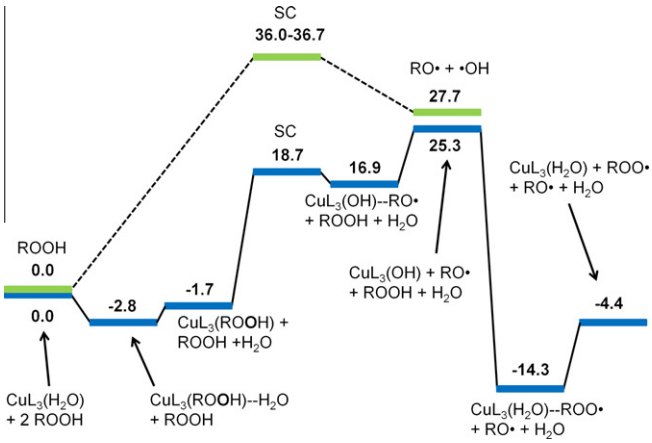

Fig. 10. Gibbs free energy along the reaction coordinate for the proposed reaction cycle over the undercoordinated copper complex (CuL_3) from Cu-MOF (blue) and oxygen–oxygen bond cleavage in the gas phase (green). All energies are in kcal/mol. (For interpretation of the references to color in this figure legend, the reader is referred to the web version of this article.)

hydroperoxide. Eventually, the RO· species departs and leaves the copper ligand cluster complexed with the ·OH species. Similar to the case of the copper paddlewheel, the Mulliken charge of the copper atom in this complex is +0.65, indicating that the copper atom has maintained a 2+ oxidation state and has not been oxidized. Next, another ROOH molecule reacts with the bound ·OH species with no barrier to produce a bound water molecule and the ROO· species (Fig. 11). The ROO· species then leaves this complex, leaving behind a water molecule bound to the paddlewheel, which completes the catalytic cycle. These calculations provide preliminary evidence that undercoordinated metal sites on the exterior surface of MOF crystals can lower the activation barrier for hydroperoxide decomposition relative to the gas-phase reaction (and relative to the liquid-phase reaction assuming negligible solvent effects). Our catalytic cycle does not include an explicit oxidation/reduction of the metal site like the Haber–Weiss cycle, but this and previous work [27,28] demonstrate that metal–hydroperoxide complexes can provide reaction pathways that catalyze hydroperoxide decomposition into free radicals. Although the choice of the undercoordinated metal cluster is certainly not unique, the results suggest that metal nodes with open coordination sites, which are not as structurally restricted as those within the interior of the MOF, may be useful hydroperoxide decomposition catalysts. It is interesting to note the similarities between the reaction coordinate of Turra et al. [28] for cobalt acetylacetonate with the one reported here for the Cu-MOF surface cluster. Certainly, it would be interesting to further investigate differences in hydroperoxide decomposition reaction mechanisms between homogeneous metal salt catalysts and metal sites on the exterior surfaces of MOFs.

4. Conclusion

Recent experiments have demonstrated that MOFs can be catalytically active materials; however, our computational results suggest that metal sites within the Co- and Cu-MOFs studied for oxidation of tetralin [24] are limited in their catalytic potential. Specifically, steric effects around metal sites may prevent direct interaction of reactants with the metal centers. Additionally, small pore sizes likely prevent diffusion of large guest molecules into the MOF. Our results suggest the possibility that surface catalysis may be dominant in these systems.

Unlike those in Co-MOF and Cu-MOF, the linkers in the copper paddlewheel structure do not sterically prevent guest molecules from forming complexes with the copper atoms. However, these clusters do not catalyze oxygen–oxygen bond cleavage of hydroperoxide species. Preliminary calculations involving undercoordinated copper clusters from Cu-MOF suggest that surface metal sites can reduce the activation barrier of hydroperoxide decomposition relative to the liquid-phase decomposition. This work represents one of the few computational efforts to investigate hydroperoxide decomposition over metal–ligand clusters—homogeneous or heterogeneous. Additional work is needed to understand these systems and to develop more active and selective oxidation catalysts in the future.

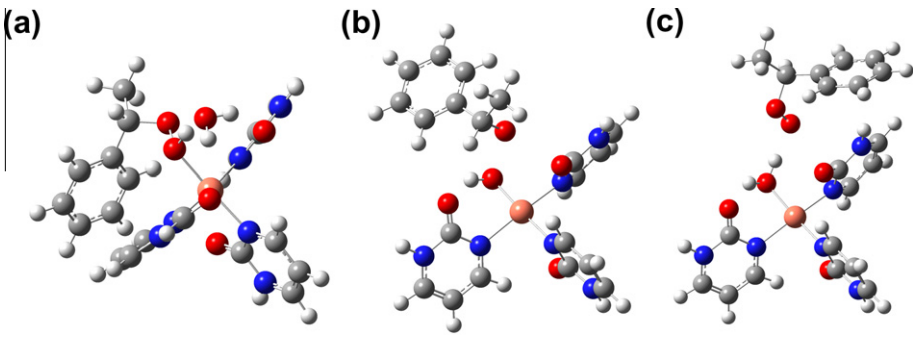

Fig. 11. Several intermediates from the surface cluster reaction coordinate: (a) $CuL_3(ROOH)–H_2O$, (b) $CuL_3(OH)–RO·$, and (c) $CuL_3(H_2O)–ROO·$.

Acknowledgments

This research was supported by a 3 M Fellowship and by the Chemical Sciences, Geosciences, and Biosciences Division, Office of Basic Energy Sciences, Office of Science, US Department of Energy Grant No. DE-FG02-03ER15457. This research used resources of the National Energy Research Scientific Computing Center, which is supported by the Office of Science of the US Department of Energy under Contract No. DE-AC02-05CH11231. The authors thank Professor Jeremy Harvey for use of his minimum energy crossing point (MECP) code.

Appendix A. Supplementary material

Supplementary data associated with this article can be found, in the online version, at doi:10.1016/j.jcat.2011.10.019.

References

[1] J.L.C. Rowsell, O.M. Yaghi, Micropor. Mesopor. Mater. 73 (2004) 3–14.
[2] G. Ferey, Chem. Soc. Rev. 37 (2008) 191–214.
[3] S. Kitagawa, R. Kitaura, S. Noro, Angew. Chem. Int. Ed. 43 (2004) 2334–2375.
[4] L. MacGillivray (Ed.), Metal-Organic Frameworks: Design and Application, Wiley, Hoboken, New Jersey, 2010.
[5] H. Li, M. Eddaoudi, M. O'Keeffe, O.M. Yaghi, Nature 402 (1999) 276–279.
[6] J.L. Rowsell, O.M. Yaghi, Angew. Chem. Int. Ed. 44 (2005) 4670–4679.
[7] M. Hirscher, B. Panella, Scripta Mater. 56 (2007) 809–812.
[8] L.J. Murray, M. Dinca, J.R. Long, Chem. Soc. Rev. 38 (2009) 1294–1314.
[9] J.R. Li, R.J. Kuppler, H.C. Zhou, Chem. Soc. Rev. 38 (2009) 1477–1504.
[10] P. Ryan, O.K. Farha, L.J. Broadbelt, R.Q. Snurr, AlChE J. 57 (2011) 1759–1766.
[11] J. Lee, O.K. Farha, J. Roberts, K.A. Scheidt, S.T. Nguyen, J.T. Hupp, Chem. Soc. Rev. 38 (2009) 1450–1459.
[12] A.M. Shultz, O.K. Farha, J.T. Hupp, S.T. Nguyen, J. Am. Chem. Soc. 131 (2009) 4204–4205.
[13] S.H. Cho, B.Q. Ma, S.T. Nguyen, J.T. Hupp, T.E. Albrecht-Schmitt, Chem. Commun. (2006) 2563–2565.
[14] D. Farrusseng, S. Aguado, C. Pinel, Angew. Chem. Int. Ed. 48 (2009) 7502–7513.
[15] A. Corma, H. Garcia, F.X. Llabrés i Xamena, Chem. Rev. 110 (2010) 4606–4655.
[16] W. Kleist, F. Jutz, M. Maciejewski, A. Baiker, Eur. J. Inorg. Chem. (2009) 3552–3561.
[17] K. Schlichte, T. Kratzke, S. Kaskel, Micropor. Mesopor. Mater. 73 (2004) 81–88.
[18] S. Choomwattana, T. Maihom, P. Khongpracha, M. Probst, J. Limtrakul, J. Phys. Chem. C 112 (2008) 10855–10861.
[19] J. Gascon, U. Aktay, M.D. Hernandez-Alonso, G.P.M. van Klink, F. Kapteijn, J. Catal. 261 (2009) 75–87.
[20] M. Banerjee, S. Das, M. Yoon, H.J. Choi, M.H. Hyun, S.M. Park, G. Seo, K. Kim, J. Am. Chem. Soc. 131 (2009) 7524–7525.
[21] G. Ferey, C. Mellot-Draznieks, C. Serre, F. Millange, J. Dutour, S. Surble, I. Margiolaki, Science 309 (2005) 2040–2042.
[22] C.Y. Sun, S.X. Liu, D.D. Liang, K.Z. Shao, Y.H. Ren, Z.M. Su, J. Am. Chem. Soc. 131 (2009) 1883–1888.
[23] M.H. Alkordi, Y.L. Liu, R.W. Larsen, J.F. Eubank, M. Eddaoudi, J. Am. Chem. Soc. 130 (2008) 12639–12641.
[24] F.X. Llabrés i Xamena, O. Casanova, R.G. Tailleur, H. Garcia, A. Corma, J. Catal. 255 (2008) 220–227.
[25] B. Moden, B.Z. Zhan, J. Dakka, J.G. Santiesteban, E. Iglesia, J. Catal. 239 (2006) 390–401.
[26] L. Gomez-Hortiguela, F. Cora, G. Sankar, C.M. Zicovich-Wilson, C.R.A. Catlow, Chem. Eur. J. 16 (2010) 13638–13645.
[27] S. Zabarnick, D.K. Phelps, Energy Fuels 20 (2006) 488–497.
[28] N. Turra, U. Neuenschwander, A. Baiker, J. Peeters, I. Hermans, Chem. – A Eur. J. 16 (2010) 13226–13235.
[29] Y. Luo, S. Maeda, K. Ohno, Tetrahedron Lett. 49 (2008) 6841–6845.
[30] K.S. Park, Z. Ni, A.P. Cote, J.Y. Choi, R.D. Huang, F.J. Uribe-Romo, H.K. Chae, M. O'Keeffe, O.M. Yaghi, Proc. Natl. Acad. Sci. USA 103 (2006) 10186–10191.
[31] L.C. Tabares, J.A.R. Navarro, J.M. Salas, J. Am. Chem. Soc. 123 (2001) 383–387.
[32] S.S.Y. Chui, S.M.F. Lo, J.P.H. Charmant, A.G. Orpen, I.D. Williams, Science 283 (1999) 1148–1150.
[33] X. Lin, I. Telepeni, A.J. Blake, A. Dailly, C.M. Brown, J.M. Simmons, M. Zoppi, G.S. Walker, K.M. Thomas, T.J. Mays, P. Hubberstey, N.R. Champness, M. Schroder, J. Am. Chem. Soc. 131 (2009) 2159–2171.
[34] A.D. Becke, Phys. Rev. A 38 (1988) 3098–3100.
[35] C.T. Lee, W.T. Yang, R.G. Parr, Phys. Rev. B 37 (1988) 785–789.
[36] W. Reints, D.A. Pratt, H.G. Korth, P. Mulder, J. Phys. Chem. A 104 (2000) 10713–10720.
[37] E.P. Clifford, P.G. Wenthold, R. Gareyev, W.C. Lineberger, C.H. DePuy, V.M. Bierbaum, G.B. Ellison, J. Chem. Phys. 109 (1998) 10293–10310.
[38] A. Schafer, C. Huber, R. Ahlrichs, J. Chem. Phys. 100 (1994) 5829–5835.
[39] R. Ditchfield, W.J. Hehre, J.A. Pople, J. Chem. Phys. 54 (1971) 724–728.
[40] A.D. McLean, G.S. Chandler, J. Chem. Phys. 72 (1980) 5639–5648.
[41] E.I. Solomon, R.K. Szilagyi, S.D. George, L. Basumallick, Chem. Rev. 104 (2004) 419–458.
[42] I. Georgieva, N. Trendafilova, L. Rodriguez-Santiago, M. Sodupe, J. Phys. Chem. A 109 (2005) 5668–5676.
[43] R. Rios-Font, M. Sodupe, L. Rodriguez-Santiago, P.R. Taylor, J. Phys. Chem. A 114 (2010) 10857–10863.
[44] M.J. Frisch, G.W. Trucks, H.B. Schlegel, G.E. Scuseria, M.A. Robb, J.R. Cheeseman, G. Scalmani, V. Barone, B. Mennucci, G.A. Petersson, H. Nakatsuji, M. Caricato, X. Li, H.P. Hratchian, A.F. Izmaylov, J. Bloino, G. Zheng, J.L. Sonnenberg, M. Hada, M. Ehara, K. Toyota, R. Fukuda, J. Hasegawa, M. Ishida, T. Nakajima, Y. Honda, O. Kitao, H. Nakai, T. Vreven, J. Montgomery, J. A., J.E. Peralta, F. Ogliaro, M. Bearpark, J.J. Heyd, E. Brothers, K.N. Kudin, V.N. Staroverov, R. Kobayashi, J. Normand, K. Raghavachari, A. Rendell, J.C. Burant, S.S. Iyengar, J. Tomasi, M. Cossi, N. Rega, N.J. Millam, M. Klene, J.E. Knox, J.B. Cross, V. Bakken, C. Adamo, J. Jaramillo, R. Gomperts, R.E. Stratmann, O. Yazyev, A.J. Austin, R. Cammi, C. Pomelli, J.W. Ochterski, R.L. Martin, K. Morokuma, V.G. Zakrzewski, G.A. Voth, P. Salvador, J.J. Dannenberg, S. Dapprich, A.D. Daniels, Ö. Farkas, J.B. Foresman, J.V. Ortiz, J. Cioslowski, D.J. Fox. 2009. Gaussian 09, Revision A.1. Gaussian, Inc., Wallingford, CT.
[45] S.F. Boys, F. Bernardi, Mol. Phys. 19 (1970) 553–566.
[46] M. Tafipolsky, S. Amirjalayer, R. Schmid, J. Phys. Chem. C 114 (2010) 14402–14409.
[47] P. Rivero, I.D.R. Moreira, F. Illas, G.E. Scuseria, J. Chem. Phys. 129 (2008) 184110.
[48] F. Illas, I.D.R. Moreira, C. de Graaf, V. Barone, Theor. Chem. Acc. 104 (2000) 265–272.
[49] J.N. Harvey, M. Aschi, H. Schwarz, W. Koch, Theor. Chem. Acc. 99 (1998) 95–99.
[50] L.D. Gelb, K.E. Gubbins, Langmuir 15 (1999) 305–308.
[51] C.D. Baertsch, H.H. Funke, J.L. Falconer, R.D. Noble, J. Phys. Chem. 100 (1996) 7676–7679.
[52] E. Haldoupis, S. Nair, D.S. Sholl, J. Am. Chem. Soc. 132 (2010) 7528–7539.
[53] T. Watanabe, S. Keskin, S. Nair, D.S. Sholl, Phys. Chem. Chem. Phys. 11 (2009) 11389–11394.
[54] J.A.R. Navarro, E. Barea, J.M. Salas, N. Masciocchi, S. Galli, A. Sironi, C.O. Ania, J.B. Parra, Inorg. Chem. 45 (2006) 2397–2399.
[55] M. Shoaee, J.R. Agger, M.W. Anderson, M.P. Attfield, CrystEngComm 10 (2008) 646–648.
[56] K. Szelagowska-Kunstman, P. Cyganik, M. Goryl, D. Zacher, Z. Puterova, R.A. Fischer, M. Szymonski, J. Am. Chem. Soc. 130 (2008) 14446–14447.